**Atmospheric
Chemistry
and Physics
Discussions**

**Chemistry of sprite
discharges**

Y. Hiraki et al.

EGU

Chemistry of sprite discharges through ion-neutral reactions

Y. Hiraki[1], Y. Kasai[2], and H. Fukunishi[3]

[1]Graduate School of Energy Science, Kyoto University, Uji, Kyoto, Japan
[2]National Inst. of Information and Communications Technology (NICT), Koganei, Tokyo, Japan
[3]Department of Geophysics, Tohoku University, Sendai, Miyagi, Japan

Correspondence to: Y. Hiraki (hiraki@center.iae.kyoto-u.ac.jp)

Abstract

We estimate the concentration changes, caused by a single streamer in sprites, of ozone and related minor species as odd nitrogen (NO_x) and hydrogen (HO_x) families in the upper stratosphere and mesosphere. The streamer has an intense electric field and high electron density at its head where a large number of chemically-radical ions and atoms are produced through electron impact on neutral molecules. After propagation of the streamer, the densities of minor species can be perturbed through ion-neutral chemical reactions initiated by the relaxation of these radical products. We evaluate the production rates of ions and atoms using electron kinetics model and assuming the electric field and electron density in the streamer head. We calculate the density variations mainly for NO_x, O_x, and HO_x species using a one-dimensional model of the neutral and ion composition of the middle atmosphere, including the effect of the sprite streamer. Results at the nighttime condition show that the densities of NO, O_3, H, and OH increase suddenly through reactions triggered by firstly produced atomic nitrogen and oxygen, and electrons just after streamer initiation. It is shown that NO and NO_2 still remain for 1 h by a certain order of increase with their source-sink balance predominantly around 60 km; for other species, increases in O_3, OH, HO_2, and H_2O_2 still remain in the range of 40–70 km. From this affirmative result of long time behavior previously not presented, we emphasize that sprites would have a power to impact on local chemistry at night. We also discuss comparison with previous studies and suggestion for satellite observations.

1 Introduction

Sprites are lightning-induced secondary discharges with both lateral and vertical scales of tens of kilometer appearing at middle atmosphere all over the world. From telescopic imaging observations it is found that the structure of the emission dominates in a cluster of thin channels with scale of 1–10 m called streamers (Gerken and Inan, 2002; Liu

and Pasko, 2004). From high temporally resolved observations it is found that the sprite streamers initiate around 60–70 km altitude and develop up to $\approx$90 km and down to 40 km with velocity of 10^7–10^8 cm/s (Moudry et al., 2003; McHarg et al., 2002). Results of spectral observations demonstrated that the emission is due to excitation of N_2(B, C) states and ionization excitation of N_2^+(A, B) through electron acceleration (e.g., Morrill et al., 2002). Streamer is a highly conducting plasma channel; as the tip propagates with high electric field and high electron density, a large amount of ions and electrons is produced and released over its path, through collisions with neutral gases (mainly N_2 and O_2) of electrons accelerated by the field. Radical particles produced, neutral atoms and excited states as well as plasmas, are considered to induce various chemical reactions. Because of no strong gas heating a technological application is expected such as reduction of toxic materials (Kulikovsky, 1997).

It has been suggested that sprites can have an impact on upper stratospheric and mesospheric ozone chemistry, which is triggered by a cluster of streamers having the above characteristics (Stenbaek-Nielsen et al., 2000; Sentman and São Sabbas, 2002; Hiraki et al., 2004; Enell et al., 2005, private communication). Here, we make a rough estimation how large impact is actually expected from generation of ions and atoms (e.g., N_2^+, N, and $O(^1D)$) through electron-molecule collision in high electric field. On the basis of laboratory and numerical studies the electron density at streamer tip is typically $n_{es} \simeq 10^{14}$ cm^{-3} being approximately uniform (e.g., Kulikovsky, 1997 and references therein). The amount of ions and atoms produced is considered to be comparable to n_{es} or larger, and is estimated to be $\approx 10^9$ cm^{-3} at altitudes of 40–50 km by assuming a scaling relation of $n_{es} \sim N^2$, N being atmospheric gas density (Pasko et al., 1998). This corresponds to $\approx$1% of ozone density at this altitude range (Brasseur and Solomon, 1986). Meanwhile, the impact on nitric oxide NO is expected to be relatively large because its ambient density is only 10 cm^{-3} or less at night. Impacts are also expected for other species as NO_2 with density of 10^8–10^9 cm^{-3} and HOx with densities of 10^4–10^7 cm^{-3}.

It is, however, not so easy to understand whether the densities of ozone, NO$_x$ (NO

and NO_2), and HO_x (H, OH, HO_2, and H_2O_2) finally increase or decrease. This is because the upper-stratospheric chemistry controlled mainly by NO_x, HO_x, and O_x (O_3 and O) is a non-linear system. NO_x and HO_x species, which destroy ozone through catalytic reactions (Brasseur, 1999), can increase by one reaction and decrease by

5 other reactions related with sprite products such as nitrogen atom N; for NO, an expected source reaction is $N+O_2 \rightarrow NO+O$ and a sink one is $N+NO \rightarrow N_2+O$. For OH, the source can be $H_2O+O(^1D) \rightarrow 2$ OH, which is a main ambient reaction in the D region, while the sink be $OH+O \rightarrow H+O_2$. In this study we perform a numerical simulation with one-dimensional ion-neutral chemical model including the effect of modeled sprite

10 streamer. The purposes are to find the way to relax of minor species after the event along with its altitude dependence and to make clear the above obscure point in the nighttime condition.

It is worthy to mention the importance of the impact on NO_x in the upper-stratosphere and mesosphere. The main ozone destroyer is generally considered to be HO_x species

15 in these regions (Brasseur, 1999). However, it is possible that NO_x supersedes HO_x as the position of ozone-reactor if its amount increases considerably through, for example, oxidation of N shown above after the occurrence of sprites. No evidence implying this enhancement has been reported because of limited spatial and temporal resolutions and sensitivity of optical instruments. Obtaining some feature from detailed

20 observation, we can suggest strongly enhanced and eccentric local chemistry above thundercloud.

2 Model description

Using an ion-neutral chemical model we calculate temporal density variations for various atmospheric species in the relaxing phase after occurrence of a sprite streamer

25 at each altitude. The reaction rate coefficients between streamer electrons and major species, N_2 and O_2, can be expressed as a function of local electric field. For simplicity not solving the streamer dynamics directly, we assume its tip field magnitude

Chemistry of sprite discharges

Y. Hiraki et al.

and its crossing time at a certain altitude and evaluate the production rates of radical particles. We consider that a reasonable evaluation of the impact as our approach will bring results of chemical model calculation with good accuracy even though the model generally has an uncertainty depending on schemes and rate coefficients.

2.1 Sprite model

Parameterization of streamer:

We suppose that the radical particles are produced predominantly at the streamer tip. We assume roughly that the tip has an impulsive electric field with a width of r_s and a uniform amplitude of E_s, and the electron density at the region being uniform as n_{es}. Here, we assume r_s being in the same order as the streamer radius (Raizer, 1991). We can consider that the lightning-induced electric field above thundercloud is directed almost vertically, and the streamer propagates along its direction with the constant velocity of v_s. Therefore, the timescale of electron acceleration, i.e. particle production, at a certain altitude is given as $t_s = r_s/v_s$. Numerical simulation results showed that E_s, n_{es}, r_s, and v_s characterizing streamer depend on boundary conditions (shapes of electrodes and applied field magnitude) and the polarity. For simplicity and maximum estimation we set as $E_s = 150$ kV/cm, $n_{es} = 10^{14}$ cm^{-3}, $r_s = 10^{-1}$ cm, and $v_s = 10^7$ cm/s taken from Kulikovsky (1997) neglecting factors of differences. These parameters are assumed to be scaled as $\sim N$, $\sim N^2$, $\sim N^{-1}$, and ~ 1, respectively, using atmospheric gas density N; for example, $r_s = 10^{-1}(N_0/N)$ cm, N_0 being the ground value, and at 70 km $r_s \simeq 10$ m, $t_s \simeq 100$ μs. We neglect here the effect of photoionization process excited through electron collisions, although it is an important process for local streamer dynamics and makes these parameters slightly shifted from the above N-scaling values (Liu and Pasko, 2004).

[EGU]

Radical products:

We assume that the accelerated electrons at the streamer tip collide only with N_2 and O_2. The collision rate coefficients k are given as a function of reduced electric field E/N through the steady-state energy distribution function of electrons along with col-
5 lision cross sections. On the basis of numerical study with a Monte Carlo technique (Hiraki et al., 2004), the relaxation time of the energy distribution is much smaller than the streamer lifetime t_s at the altitude of our interest, and the major composition of at-mosphere changes hardly in the timescale of t_s. In what follows, the production rate of a particle j is given constantly as $P_j = k_j(E_s/N)Nn_{es}$ all through the streamer propaga-
10 tion. We obtain the electron energy distribution function with a Monte Carlo technique. Here we take the cross sections of e-N_2, O_2 collisions from updated compilation by Itikawa (2006, 1994), respectively. We consider, as radical particle j, atoms of O(^{1}D), O(^{3}P), N(^{4}S), and N(^{2}D), and adopt the cross section data in Cosby (1993a, b) and Itikawa (1994); the excited species of $O_2(a^1\Delta_g)$ and $N_2(A^3\Sigma_u^+)$ and ionic species of O^+,
15 O_2^+, O^-, N^+, and N_2^+ are considered with including cascade effects from O_2(b), N_2(B, C), O_2^+(a, b, A), and N_2^+(A, B). Cross sections for all these particles are taken from Itikawa (1994, 2006). We disregard other possible source processes. We obtain the most reliable set of production rates especially for atomic nitrogen and oxygen of criti-cal importance in the following calculation by recalculating electron energy distribution
20 with updated cross sections of N_2 by Hiraki and Fukunishi (2006).

2.2 Chemical model

We represent the chemical impact of the sprite streamer with two parameters P_j and t_s, both of which are only functions of altitude through N. We estimate composition changes at altitudes of 40–90 km using one-dimensional chemical model after occur-
25 rence of the modeled streamers at each altitude. We adopt basically the chemical model of neutral atmosphere by Iwagami et al. (1998). This model treats 40 neutral species including O_2(a), O(^{1}D), O(^{3}P), and N(^{4}S) shown above, and covers the altitude

range of 0–90 km; reaction coefficients are taken from DeMore et al. (1994). We include thermal electrons and 34 ionic species such as $O_i^\pm$, N_i^+, and $NO_i^\pm$ (i≤4) into the above model on the basis of reaction data by Ogawa and Shimazaki (1975), Borisov et al. (1993), Rees (1989), Brasseur and Solomon (1986), Tochikubo and Arai (2003), and Matzing (1991).

In order to obtain a reference diurnal density variation used for initial values we make firstly a temporal integration (hundreds of days) of rate equations $d_t n = P - L n$ of all ions and neutrals at altitudes of 0–90 km with the day of year and moderate solar activity being fixed on the basis of Iwagami et al. (1998). Here we include the vertical eddy and molecular diffusions for neutral species. Adding the production terms P_j of radical particles and using the reference density data at an arbitrary local time t_0, we solve rate equations for all species separately without assumption of families until the time $t = t_0 + t_{relax}$ by an implicit method. It is noted that the sprite impacts P_j are non-zero at each altitude at $t \leq t_s$. Here we disregard the vertical diffusion term in order to focus the streamer effect on each-altitude local chemistry. The altitude interaction makes no sense because the initiation of actual streamer at all altitudes does not coincide at t_0. The electron temperature, used for calculation of reaction coefficients, is assumed to be 10 eV at the period of $t_0 < t < t_0 + t_s$, after which it equals to the neutral temperature, while the ion temperature is not perturbed at all. We assume the neutral temperature unchanged from the ambient values because Joule heating by sprite discharge may be negligibly small. One can estimate the secondary sprite impact at the same site using the same initial density data because the air parcel with composition change by primary sprite is advected to other site by a horizontal wind. Hereafter, we redefine $t = t_0$ as $t = 0$.

3 Numerical simulation and results

We focus the chemical impact of sprites in the nighttime stratosphere and mesosphere where most of events are observed. In this paper we estimate only the impact of

streamer head where large amount of radical particles are produced in strong electric field. We show first in Fig. 1 the production rate coefficients of $N(^4S)$, $N(^2D)$, $O(^3P)$, and $O(^1D)$ atoms through electron impact dissociations of molecular nitrogen and oxygen calculated with a Monte Carlo method. Streamer electric field, 150 kV/cm at ground level, corresponds to a reduced value of E/N=600 Td; in this field the average electron energy $\approx$12 eV exceeds dissociation limit. The coefficients of the above atomic production and ionization show the largest values at this field among inelastic processes such as metastable-state excitation. It is also found that these values are much larger than a typical ion-molecular reaction coefficient ($\approx 10^{-10}$ cm^{-3} s^{-1}) in the atmosphere. It is clear from a simple estimation that the amount of produced N atom written as $k_{\mathrm{diss}} N n_{\mathrm{es}} t_s$ overwhelms the ambient one, which is negligibly small below 70 km altitude: $k_{\mathrm{diss}} \approx 5 \times 10^{-9}$ cm^3 s^{-1}, $n_{\mathrm{es}} = 10^{14} (N/N_0)^2$ cm^{-3}, and $t_s = 10^{-8} (N_0/N)$ s. Furthermore it is in the same order or exceeds the nighttime NO density at altitude range of 40–70 km.

We solve rate equations to calculate the density changes for various species when a single streamer effect as source term $P = k_i N n_{\mathrm{es}}$ is given at altitudes of 40–90 km. Here we assume the fixed conditions such as temperature being at mid-latitude equinox (Iwagami et al., 1998). Firstly, we show in Fig. 2 the density distributions of NO$_x$ (NO and NO$_2$) species one second and one hour after initiation of a single streamer. We find that the NO density increases strongly at t=1 s, whereas NO$_2$ does not change so much except below 55 km since NO$_2$ is abundant as NO$_x$ below 70 km at night, and above the altitude the sprite impact itself is too small. We find that a decrease of NO$_2$ below 55 km is due to negative-ion reactions related with strongly enhanced N, O, and NO. The key reactions of increase in NO density (up to 10^{11} cm^{-3} at $t \leq 1$ s) are electron impact dissociation of N$_2$ and oxidation of N atom as a series below,

$$N_2 + e \rightarrow N(^4S) + N(^2D) + e \tag{R1}$$

$$N + O_2 \rightarrow NO + O. \tag{R2}$$
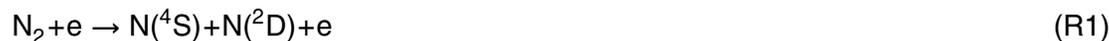
This response is consistent with the maximum production of N, $P_{\mathrm{diss}} t_s \approx 1.2 \times 10^{12}$ cm^{-3} at 40 km. The saturation around 40 km is caused by the NO$_x$ reduction process as

2318

N+NO→N$_2$+O. Note that the N atoms in the second equation are mostly in the state of ^{4}S, while the excited state ^{2}D is already lost at all at this moment. It is, however, confirmed that the effect on NOx species continues over 1 s in spite of assumed lifetime of sprites less than 1 ms (maximum at 90 km). The increasing rate of NO is the order of 10^5–10^9 at altitude range of 40–70 km. We would investigate the response at 1 h after the event, even if it is an order-estimation, in order to discuss the effect on atmospheric chemistry. The noticeable enhancements sustain around 60 km altitude for NO and 40–60 km for NO$_2$ (Fig. 2). Especially, we show in Fig. 3 the time variation in NO and NO$_2$ densities at 60 km. We find from this figure and by checking dominant reactions that NO sustains its amount through the relaxation of ions and atoms as N at the initial phase ($t \leq 100$ s), after that, almost all convert to NO$_2$ through the following processes:

$$NO + O_3 \rightarrow NO_2 + O_2 \tag{R3}$$

$$NO + O + M \rightarrow NO_2 + M \tag{R4}$$

$$NO + HO_2 \rightarrow NO_2 + OH. \tag{R5}$$

This is because the response of NO$_2$ is in anti-phase to NO, resulting in the remarkable increase at t=1 h. On the other hand, it is confirmed that the dominant loss reactions of NO$_2$ are NO$_2$+O→NO+O$_2$ and NO$_2$+H→NO+OH. Thus, the loss rate of NO becomes relatively small around 60 km due to the source-sink balance in NO$_x$ as the above five reactions. Contrary to the linear response to sprite impact at t=1 s, these particles are strongly coupled each other along with weak couplings with O$_x$ and HO$_x$ in this timescale. It is mentioned that the final sink of NO$_x$ to sprite impact is NO$_2$, which has a large lifetime; its density amounts to $\approx 6 \times 10^9$ cm^{-3} at 40 km. The increasing rates at t=1 h are summarized as, for NO, up to the order of 6 with its maximum around 60 km, while, for NO$_2$, the order of 1 at the range of 40–60 km. We emphasize from this result that the impact can sustain for a few hours. In addition to the above key reactions ineffectiveness of the reaction N+NO→N$_2$+O has a critical role because the impact will diminish perfectly if this reaction rate is so fast. It is slightly seen as a saturation

Chemistry of sprite discharges

Y. Hiraki et al.

EGU

of the increasing rate of NO_2 at $t=1$ h at 40 km. However, we can interpret that the conversion of $N \rightarrow NO \rightarrow NO_2$ is smoothly proceeded in a scale of 1 h with negligible contribution of this reaction since the production rate of N atom is smaller at higher altitude and its loss timescale is smaller at lower altitude (≈ 1–10 s). We also confirmed that the contribution of ion-molecular reactions to the NO_x chemistry is restricted within $t=1$–10 s and do not work at all at $t=1$ h.

Next we show density distributions of O_x (O and O_3) at $t=1$ s and 1 h in Fig. 4, and these temporal variations at 40 km in Fig. 5. The excited state $O(^1D)$ diminishes at all within 1 s through dissociation of H_2O and ion-molecular reactions, although the amount of production is the same order as $O(^3P)$. For O and O_3, the response is relatively simple, i.e. linear to the sprite impact ($\sim N$), except for some contributions to other species such as loss of NO_2 by O and destruction of HO_2 and OH (see next paragraph). It is summarized that the O atom increases firstly and then O_3 increases as the following series of key reactions;

$$O_2 + e \rightarrow O(^1D) + O + e \qquad \text{(R6)}$$

$$O + O_2 + M \rightarrow O_3 + M. \qquad \text{(R7)}$$

These processes (conversion of $O \rightarrow O_3$) are considered to occur below 70 km. Figure 5 clearly shows that the final sink of O_x to sprite impact is O_3, while O decreases in a scale of $<10^3$ s. Consequently, the increasing rate of O_3 by a single sprite streamer becomes maximum at 40 km being up to the factor of 4; its density amounts to $\approx 2 \times 10^{12}$ cm^{-3}. Because the maximum production of O and $O(^1D)$ is $P_{diss} t_s \approx 5 \times 10^{11}$ cm^{-3} through the process (R6), other processes such as ionization (O_2^+, O^+) and excitation ($O_2(a)$) of O_2, and process (R2) also have large contribution to the ozone production within a scale of 1–100 s.

Next we show density distributions of HO_x (H, OH, HO_2, and H_2O_2) at $t=1$ s and 1 h in Fig. 6, and these time variations at 40 km and 60 km in Fig. 7. The response of HO_x is found to be more complicated and unexpected than those of other species NO_x

EGU

and O_x. We investigate firstly the main trigger reaction of HO_x density changes within $t = 1$ s at 40 km where atomic hydrogen H and hydroxyl radical OH increase strongly with a nearly linear dependence on sprite impact. Contrary to our expectation that the sprite-produced $O(^1D)$ contributes mainly through the reactions $H_2 + O(^1D) \rightarrow H + OH$ and $H_2O + O(^1D) \rightarrow 2OH$ as similar to lower-thermospheric chemistry, more contribution is made by produced electrons through the following reactions up to the time of 1 ms:

$$H_3O^+OH + e \rightarrow H + OH + H_2O \tag{R8}$$

$$HNO_3 + e \rightarrow OH + NO_2^-. \tag{R9}$$

Thus both H and OH increase exclusively. However, these reactions concede position of a main trigger to the following ones through relaxations of ions and electrons to the initial densities until $t \approx 1$ s,

$$H + O_3 \rightarrow OH + O_2 \tag{R10}$$

$$HO_2 + O \rightarrow OH + O_2 \tag{R11}$$

$$OH + O \rightarrow H + O_2, \tag{R12}$$

showing a successive multiplication. In addition, Fig. 6 shows that increases in HO_2 by the order of 1–4 in the range of 40–55 km and in H_2O_2 by several factors in the range of 55–65 km follow. We would mention briefly the difference of the latter two particles' responses at $t \approx 1$–100 s. We confirmed that HO_2 is produced with not only oxidation of H and OH but destruction of H_2O_2 by O, OH, and H. A large increase in HO_2 at 40 km is due to considerable increases in H and OH, whereas the rate becomes smaller in upper altitude, substituted for the production of H_2O_2. A relatively small but constant increase in H_2O_2 around 40–70 km is due mainly to non-linear reactions of $HO_2 + HO_2 \rightarrow H_2O_2 + O_2$ and $OH + OH + M \rightarrow H_2O_2 + M$. Figure 7 also show that in a timescale of ≈ 100 s firstly almost all H, with small intrinsic lifetime, converts to OH and HO_2, followed by a large increase in H_2O_2 through destructions of these two particles,

EGU

mainly OH having fast relaxation time at 40 km and enhancement at 60 km. At $t=1$ h the increasing rate of H_2O_2 at 40 km is finally the order of ≈ 1; its density amounts to $\approx 7 \times 10^7$ cm^{-3}. Around 60 km altitude, the increasing rate shows similar tendency in spite of slow reduction rate of OH due to slow relaxation of H. It is summarized that the final sinks to the sprite impact are HO_2 and H_2O_2 at 40 km with increasing rates by the order of 3 and 1, respectively, while are OH and H_2O_2 at 60 km with those by the order of 2 and 1, respectively, where HO_2 relaxes within $t \approx 10^3$ s.

We tried to interpret roughly the longtime behaviors over 100 s in HO_2 and H_2O_2 with steady-state formulation. We find that the source reactions of HO_2 are mainly those of OH with O_3 and H_2O_2, while its loss reaction is concerned with NO_x (NO, NO_2); its density can be approximately written as $[HO_2] \propto (\Delta[O_3]+\Delta[H_2O_2])/\Delta[NO_x]$, assuming variable terms dominant. The HO_2 density would not change largely around 60 km because of rapid reduction of NO, no increase of NO_2 ($\approx 10^3$ s), and moderate increases of O_3 and H_2O_2 (see Figs. 2 and 4). Over the altitude, Δ [NO] is still effective to cause its decrease. It increases in the range of 40–50 km in accord with increases of O_3 and H_2O_2, more effective than that of NO_2 relating three-body reaction with HO_2, where NO already relaxes. On the other hand, the source reactions of H_2O_2 are mainly reactions of OH×2 or HO_2×2 shown above, while its loss reaction is concerned with OH; the loss processes by O and H atoms, perfectly relaxing, do not contribute so much. Its density increases at both 40 and 60 km with increasing OH due to predominance of non-linear term, i.e. $[H_2O_2] \propto \Delta[OH]$, after which it saturates by linear terms as $[H_2O_2] \propto \Delta$ $[HO_2]/\Delta[OH] \approx$ const at 40 km and $\propto \Delta[OH]/\Delta$ [OH] $\approx$ const at 60 km (here Δ $[HO_2] \approx 0$).

We would discuss possible uncertain factors for our calculation shown above even though it is only an order-estimation: (i) accuracy in molecular chemical reaction coefficient, (ii) uncertainty in the streamer-tip electric field magnitude, and (iii) contribution of the other part of streamer (i.e. body, or bead-structure). (i) We firstly compare reaction rate coefficients we use with newer ones. In the above discussion, the key reactions for NO_x chemistry is Reaction (R2) as a trigger (NO being secondary

EGU

product), Reactions (R3)–(R5) (sink to NO_2), and $N+NO \rightarrow N_2+O$; these are Reaction (R7) for O_x, H_2 (H_2O)+$O(^1D) \rightarrow H+OH(2OH)$ and Reactions (R10)–(R12) as triggers, $OH+OH+M \rightarrow H_2O_2+M$ and $HO_2+HO_2 \rightarrow H_2O_2+O_2$ etc. for HO_x. We referred to the compiled data of DeMore et al. (1994) for these reaction coefficients. Comparing
5   their updated data of Sander et al. (2006), almost all of the above NO_x and O_x reactions are unchanged except for Reaction (R3) having a difference of <1% at 250 K, while for HO_x the difference is less than 30% at 250 K. From these facts we consider that uncertainty in rate coefficients is under our estimation.

    (ii) Next, we perform a response study how much the results vary with the streamer
10   electric field value. When the field value is set to be in the range of 400–800 Td, the NO density at $t=1$ h varies in the scale of 1 order around the value in Fig. 2. However, our conclusion remains essentially unchanged because the difference is found to be almost linear to the amount of first product, i.e. k. Here it is difficult to mention the details about the effect on other species with their increasing scales of 1–2 orders,
15   which is the same order as the above uncertainty. (iii) We focus in our model only the impact of the streamer tip with strong electric field. It is suggested that the tail part is actually formed after the tip passes away, in which a slight-amplitude electric field exists despite not causing strong electron acceleration and optical emission (Liu and Pasko, 2004); ≥ 60 Td. From optical measurement of sprites, the bead-like structures
20   with strong emissions are found to be formed in the region a cluster of streamers exists (Gerken and Inan, 2002; Moudry et al., 2003). Both lifetimes are in the order of ≈ 1– 10 ms. We guess in this paper that the former effect is negligibly small and the latter one cannot be evaluated because of lack of its mechanism to date; these should be done in our future studies. Our some speculation to this problem is made as follows.
25   We consider that the predominantly produced particles in streamer tail are metastable states such as $N_2(v=1)$ and $N_2(A)$ rather than N and O atoms of great importance in our calculations. As a mechanism, the multiple excitation is needed to gain dissociation energy and to cause the density variation of NO_x and HO_x triggered by these particles; the highly excited secondary and ternary products dissociate N_2 and H_2. However,

EGU

these processes are expected not to be so dominant in our transient discharge with small lifetime and small particle production, different from stable glow discharge.

4 Discussion

On the basis of our calculation results we try to evaluate roughly the sprite impact on local chemistry at nighttime. Here we examine whether the mean density variation for a certain species survives or not when the impact is mixed in a local area as a similar approach by Hiraki et al. (2004). We focus nitric oxide NO of the most possible one. The variation in the NO density by a single streamer is over the order of 6 at 60 km altitude. Here we assume the horizontal scale of sprites with a cluster of streamers being 100 km^2 at their maximum. The local area is defined to be 10^6 km^2 as the resolution of some satellite, e.g. Envisat-Sciamachy (limb emission sounder), in which the increasing rate of NO is reduced as $1/10^4$ through mixing without any loss. However, our calculated variation can survive evidently with the order of 2 in spite of the wide-range mixing. Our estimation being only for one event, the impact is expected to be larger in the area such as Africa where many events of lightning and sprites are possible within several hours. It is also expected to be still large even though this kind of estimation depends certainly on the initial condition; we discuss this point in the next paragraph. We emphasize that the density increase of at least NO is detectable if a certainly resolved and qualified observation is performed. Note that this discussion is limited in the nighttime impact because the daytime ambient density of NO becomes, through photolysis of NO_2, the same order as that produced by one streamer event at night. It is one of future studies of this field whether integration of nighttime local variation in NO_x by many sprite events affects on these diurnal variations. We would suggest some ideas to the future observational studies including this point. Our estimation is done on purpose to determine the upper limit with uncertainty in a few orders due to streamer electric field and scale parameters so that it needs verification with observation. Since the sprite impact on chemical species vary widely with altitude, sub-millimeter wave

limb emission sounders such as Envisat-Sciamachy and ODIN-SMR are adequate to detect it; these probes measure the densities of NO, NO_2, and O_3 above 40 km altitude with moderate accuracy, which is comparable with our results. A thorough comparison can be done if high-quality data is obtained from the measurements at nighttime or pre-dawn. It is also hoped that, if the horizontal resolution becomes smaller than 1000 km, detectable limit becomes higher and traces in several particles except NO such as O_3 and OH can be achieved.

Finally we compare our calculation results with other studies. To date the similar calculation is done by Enell et al. (2005). They showed the increasing rate of the NO density after initiation of a sprite streamer in the nighttime condition at equator (in summer and low solar activity). The increasing rate is the order of 2–3 at 40–50 km at its maximum, and no increase is seen above the altitude range. They also show the longtime behavior that the NO density relaxes to the initial value within 1 h. The response at this altitude range is very similar to our results, however, that above the altitude is quite different. We elaborate to mention the response around 60 km, being important in the viewpoint of atmospheric chemistry, where in our case the rate is instantaneously the order of 6. The difference in this rate is undoubtedly due to the difference in the evaluation of sprite first products as input parameters. It remembers that we give altitude dependence of the production rate on the basis of scaling law of streamer dynamics and include all possible particles produced through e-N_2, O_2 inelastic collisions. On the other hand, Enell et al. (2005) considered only some N_2 excited states and N_2^+ identified from recent optical measurements, not including N and O atoms, which are of great importance in our calculation results. Furthermore, the magnitude itself of their particle production is considerably smaller than ours. It would be due to the time averaging effect on the measurement of streamer emission intensity, causing an underestimation of the production rates derived. We additionally mention dependence of the results on the initial values of chemical model adopted. At 60 km the initial value of NO density is in our case $\approx 10^2$ cm^{-3}, while in theirs $\approx 10^6$ cm^{-3}. It is not clear in details but the difference is considered to be due to the difference in the

Chemistry of sprite discharges

Y. Hiraki et al.

EGU

referring latitude and data set of reaction rate coefficients. It is, however, asserted that the increasing rate of NO density in the order of 2–3 would be obtained if we calculate with their initial values, and be detectable with satellite sounder observations if 100 sprites occur within 1 hour, as discussed in the above paragraph.

5 Summary

We investigate density variations of NO_x, O_x, and HO_x species after the initiation of a single sprite streamer using a specified ion-neutral chemical model with modeling chemically radical particle production by non-thermal electrons. Results show that the densities of NO, O_3, OH, and H rapidly increase, by the orders up to 8 for NO and H while several orders for other two, through reactions triggered by sprite first products as O, N, and electrons in the timescale of 1–10 s at nighttime. It is demonstrated that the impacts sustain over one hour, especially for NO the increasing rate still being the order of 6 around 60 km altitude. The final sinks are considered to be NO_2, O_3, HO_2, and H_2O_2 for each species with increasing rates by several orders. These long lifetime responses are related with source-sink balances of NO-NO_2 and of HO_2-H_2O_2 newly constructed by sprite products. We suggest that the sprite impact on these minor species will be detectable with highly qualified satellite observations, even though it has an uncertainty by ≈ 1 order due to initial conditions and magnitudes of particle production.

References

Borisov, N. D., Kozlov, S. I., and Smirnova, N. V.: Changes in the chemical composition of the middle atmosphere during multiple microwave pulse discharge in the air, translated from Kosm. Issled., 31, 63–74, 1993.

5   Brasseur, G.: Atmospheric chemistry and global change, Oxford Univ. Press, New York, 1999.

Brasseur, G. and Solomon, S.: Aeronomy of the Middle Atmosphere, 2nd ed., D. Reidel, Norwell, Mass, 1986.

Cosby, P. C., Electron-impact dissociation of nitrogen, J. Chem. Phys., 98, 9544–9553, 1993a.

Cosby, P. C., Electron-impact dissociation of oxygen, J. Chem. Phys., 98, 9560–9569, 1993b.

10   DeMore, W. B., Golden, D. M., Hampson, R. F., Howard, C. J., Kurylo, M. J., Molina, M. J., Ravishankara, A. R. , and Sander, S. P.: Chemical Kinetics and Photochemical Data for Use in Stratospheric Modeling, Evaluation, Number 11, JPL Publication 94-26, Jet Propulsion Laboratory, California Institute of Technology, Pasadena, CA, 1994.

Enell, C.-F.,Verronen, P. T., Seppälä, A., Turunen, E., and Ulich, T.: Possibility of NO production

15   by transient luminous events studied in a coupled ion-neutral chemical model, 9th IAMAS Assembly, Beijing, 2005.

Gerken, E. A. and Inan, U. S.: A survey of streamer and diffuse glow dynamics observed in sprites using telescopic imagery, J. Geophys. Res., 107(A11), 1344, doi:10.1029/2002JA009248, 2002.

20   Hiraki, Y., Tong, L., Fukunishi, H., Nanbu, K., Kasai, Y., and Ichimura, A.: Generation of metastable oxygen atom $O(^1D)$ in sprite halos, Geophys. Res. Lett., 31, L14105, doi:10.1029/2004GL020048, 2004.

Hiraki, Y. and Fukunishi, H.: Theoretical criterion of charge moment change by lightning for initiation of sprites, J. Geophys. Res. 111, A11305, doi:10.1029/2006JA011729, 2006.

25   Itikawa, Y.: Electron collisions with N_2, O_2, and O: what we do and do not know, Adv. Atom. Mol. Opt. Phy., 33, 253–274, 1994.

Itikawa, Y.: Cross sections for electron collisions with nitrogen molecules, J. Phys. Chem. Ref. Data, 35, doi:10.1063/1.1937426, 2006.

Iwagami, N., Inomata, S., and Ogawa, T.: Doppler detection of hydroxyl column abundance in

30   the middle atmosphere: 2. measurements for three years and comparison with a 1-D model, J. Atmos. Chem., 29, 195–216, 1998.

Chemistry of sprite discharges

Y. Hiraki et al.

Title Page

Abstract	Introduction
Conclusions	References
Tables	Figures

◄◄   ►►

◄   ►

Back   Close

Full Screen / Esc

Printer-friendly Version

Interactive Discussion

EGU

Kulikovsky, A. A.: Production of chemically active species in the air by a single positive streamer in a nonuniform field, IEEE Trans. Plasma Sci., 25, 439–446, 1997.

Liu, N. and Pasko, V. P.: Effects of photoionization on propagation and branching of positive and negative streamers in sprites, J. Geophys. Res., 109, A04301, doi:10.1029/2003JA010064, 2004.

Mätzing, H.: Chemical kinetics and flue gas cleaning by irradiation with electrons, Adv. Chem. Phys., 80, 315–402, 1991.

McHarg, M. G., Haaland, R. K., Moudry, D. R., and Stenbaek-Nielsen, H. C. : Altitude-time development of sprites, J. Geophys. Res., 107(A11), 1364, doi:10.1029/2001JA000283, 2002.

Morrill, J. S., Bucsela, E. J., Siefring, C., Heavner, M. J., Berg, S. L., Moudry, D. R., Slinker, S., Fernsler, R., Wescott, E. M., Sentman, D. D., and Osborne, D.: Electron energy and electric field estimates in sprites derived from ionized and neutral N_2 emissions, Geophys. Res. Let., 29(10), 1462, 10.1029/2001GL014018, 2002.

Moudry, D. R., Stenbaek-Nielsen, H. C., Sentman, D. D., and Wescott, E. M.: Imaging of elves, halos and sprite initiation at 1 ms time resolution, J. Atmos. Solar-Terr. Phys., 65, 509–518, 2003.

Ogawa, T. and T. Shimazaki: Diurnal variations of odd nitrogen and ionic densities in the mesosphere and lower thermosphere: simultaneous solution of photochemical-diffusive equations, J. Geophys. Res., 28, 3945–3960, 1975.

Pasko, V. P., Inan, U. S., and Bell, T. F.: Spatial structure of sprites, Geophys. Res. Lett., 25, 2123–2126, 1998.

Raizer, Y. P.: Gas Discharge Physics, 1st ed., Springer-Verlag, New York, 1991.

Rees, M. H.: Physics and chemistry of the upper atmosphere, Cambridge university press, Cambridge, 1989.

Sander, S. P., Finlayson-Pitts, B. J., Friedl, R. R., Golden, D. M., Huie, R. E., Keller-Rudek, H., Kolb, C. E., Kurylo, M. J., Molina, M. J., Moortgat, G. K., Orkin, V. L., Ravishankara, A. R., and Wine, P. H.: Chemical Kinetics and Photochemical Data for Use in Atmospheric Studies, Evaluation Number 15, JPL Publication 06-2, Jet Propulsion Laboratory, Pasadena, 2006.

Sentman, D. D. and São Sabbas, F. T.: Energy deposition of sprites in the middle-upper atmosphere, 3rd Brazilian Workshop on Atmospheric Electricity, Brazil, 2002.

Stenbaek-Nielsen, H. C., Moudry, D. R., Wescott, E. M., Sentman, D. D., and São Sabbas, F. T.: Sprites and possible mesospheric effects, Geophys. Res. Lett., 27, 3829–3832, 2000.

EGU

Tochikubo, F. and Arai, H.: Numerical simulation of streamer propagation and radical reactions in positive corona discharge in N_2/NO and N_2/O_2/NO, Jpn. J. Appl. Phys., 41, 844–852, 2002.

EGU

EGU
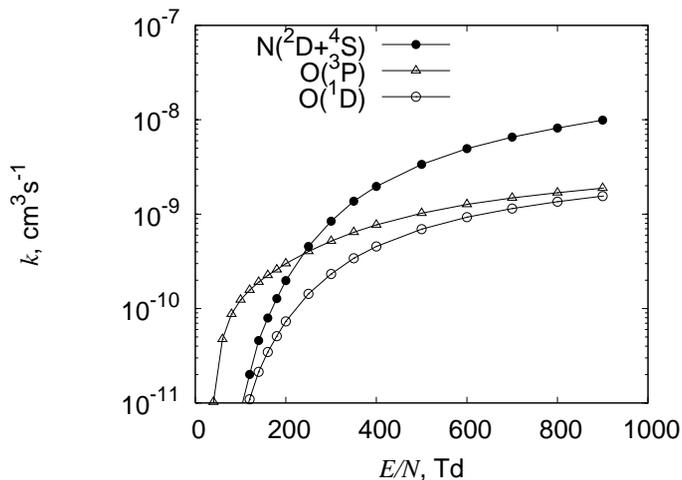
Fig. 1. Rate coefficients k of electron impact dissociative excitations of N_2 and O_2 as a function of reduced electric field E/N; we use cross sections for the fragments of $N(^2D)+N(^4S)$, $O(^3P)+O(^3P)$ (the lower threshold), and $O(^3P)+O(^1D)$, and multiply the mixing ratio as $N_2:O_2=0.8:0.2$ for illustration.
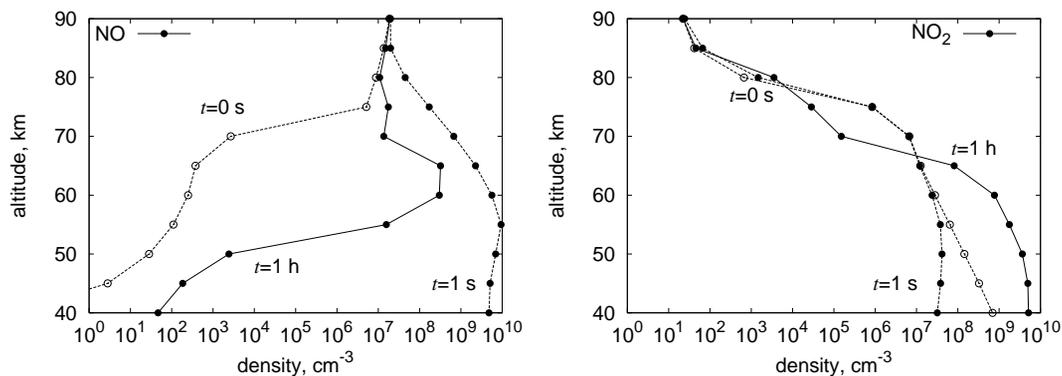
Fig. 2. The density variations for NO_x (NO and NO_2) species at the periods of $t=1$ s (dashed lines with closed circles) and 1 h (solid lines) after the initiation of a sprite streamer ($t=0$) at the nighttime condition, dashed lines with open circles showing these initial values.

EGU
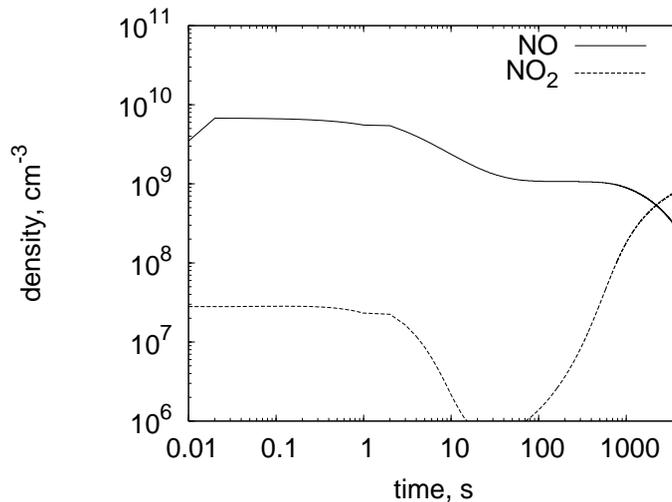
Fig. 3. Temporal density variations for NO_x species at 60 km altitude in the same condition as Fig. 2; solid and dashed lines show those of NO and NO_2, respectively, after initiation of streamer at $t=0$.
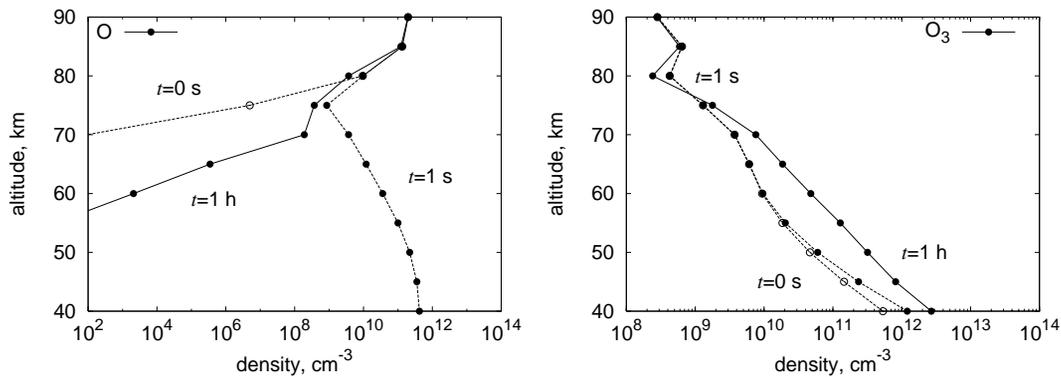
Fig. 4. Same as Fig. 2, but shown are for O_x ($O(^3P)$ and O_3) species.

ACPD

8, 2311–2336, 2008

Chemistry of sprite discharges

Y. Hiraki et al.

Title Page

Abstract | Introduction

Conclusions | References

Tables | Figures

◄◄ | ►►

◄ | ►

Back | Close

Full Screen / Esc

Printer-friendly Version

Interactive Discussion

EGU

EGU
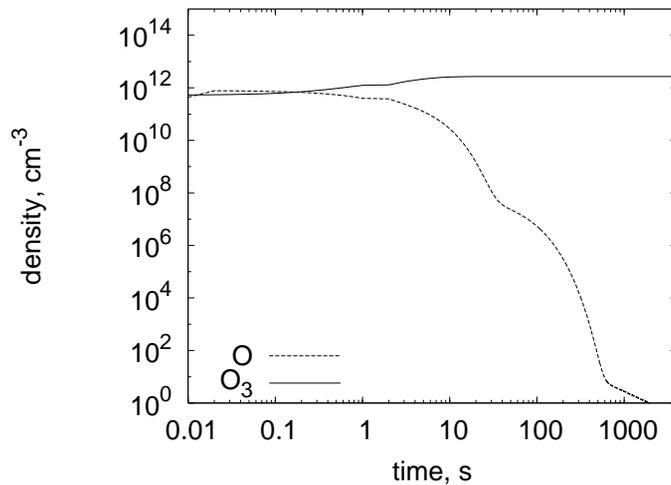
Fig. 5. Temporal density variations for O_x species at 40 km in the same condition as Fig. 4; solid and dashed lines show those of O_3 and O, respectively.
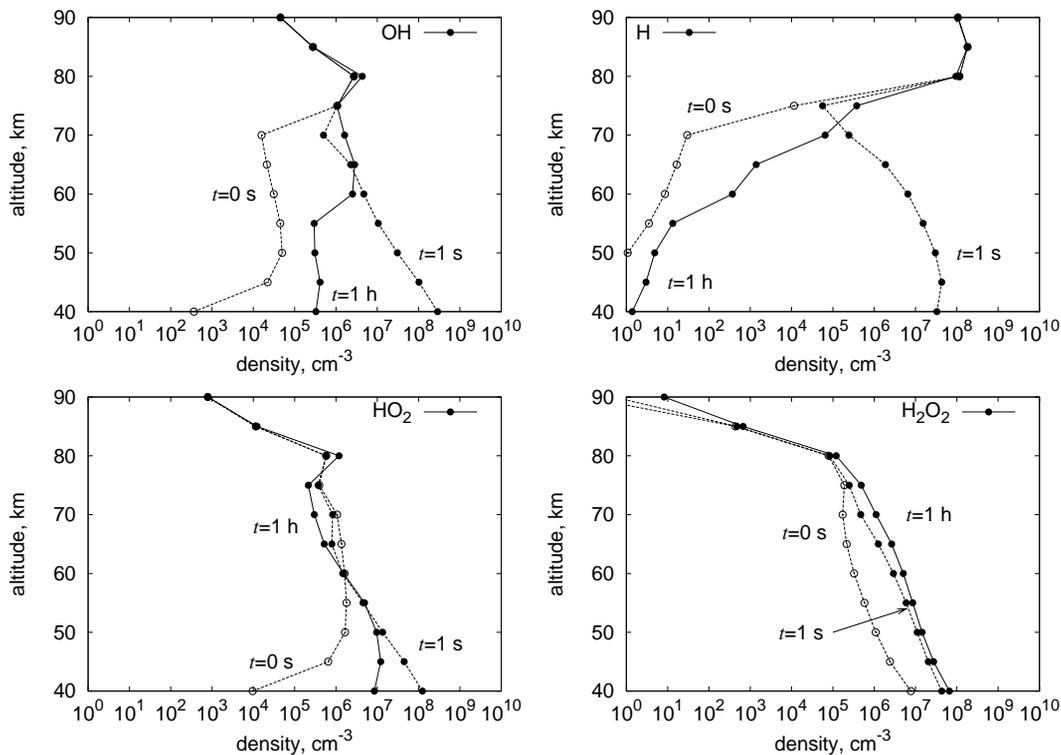
Fig. 6. Same as Fig. 2, but shown are for HO_x (OH, H, HO_2, and H_2O_2) species.

ACPD

8, 2311–2336, 2008

Chemistry of sprite discharges

Y. Hiraki et al.

Title Page

Abstract | Introduction

Conclusions | References

Tables | Figures

◄◄ | ►►

◄ | ►

Back | Close

Full Screen / Esc

Printer-friendly Version

Interactive Discussion

EGU

EGU
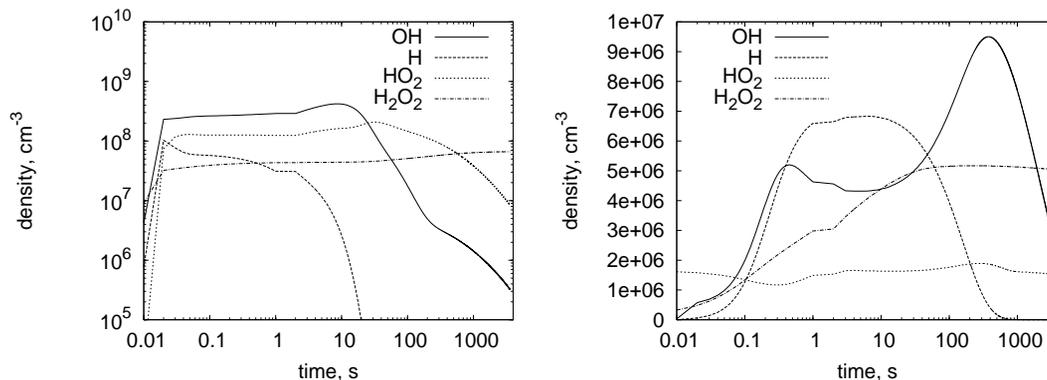
Fig. 7. Temporal density variations for HO_x species at 40 km (left panel) and 60 km (right panel) in the same condition as Fig. 6; solid, dashed, dotted, and dashed-dotted lines show those of OH, H, HO_2, and H_2O_2, respectively.